Snowball Earth transitions from Last Glacial Maximum conditions provide an independent upper limit on Earth's climate sensitivity

Martin Renoult[1,2,3], Navjit Sagoo[2,3], Johannes Hörner[4], and Thorsten Mauritsen[2,3]

[1]Department of Geological Sciences, Bolin Centre for Climate Research, Stockholm University, Stockholm, Sweden

[2]Bolin Centre for Climate Research, Stockholm University, Stockholm, Sweden

[3]Department of Meteorology, Stockholm University, Stockholm, Sweden

[4]Department of Meteorology and Geophysics, University of Vienna, Vienna, Austria

Correspondence: Martin Renoult (martin.renoult@misu.su.se)

Abstract. Geological evidence of a snowball Earth state indicate persistent tropical sea ice cover during the Neoproterozoic (>635 million years ago). Current theory is that a strengthening of the positive surface albedo feedback with cooling temperatures, eventually exceeding the sum of all other feedbacks, leads to a global climate instability. Several recent high sensitivity climate models with strongly positive cloud feedbacks have not been able to simulate the much warmer Last Glacial Maximum (LGM) state, suggestive that they cool excessively in response to a modest decrease in atmospheric carbon dioxide levels and therefore enter the snowball instability by this mechanism. Using a coupled Earth system model, MPI-ESM1.2, we show that clouds accelerate the transition to a snowball Earth state and reduce the radiative forcing required to trigger the climate instability. Positive cloud feedbacks over tropical oceans and ahead of the sea-ice edge act to cool down the oceans and promote sea ice formation. Regardless, when approached slowly the snowball Earth transitions appear to occur around a global mean temperature of zero degree Celsius, simultaneously with the sea ice edge advancing into the sub-tropics thereby strengthening the surface albedo feedback. This temperature threshold, if supported by several climate models, could be used as a novel and independent constraint on the upper bound of climate sensitivity by using the relationship of simulated LGM temperatures and the models' equilibrium climate sensitivity, combined with the simple fact that Earth did not enter a snowball instability during the recent ice ages. Currently, using the ~~results from MPI-ESM1.2~~here estimated transition temperature, we find it is implausible that Earth's climate sensitivity exceeds ~~5.5 K (4.4~~ 6.2 K (3.9 – ~~6.6~~8.4, 90 percent confidence).

1 Introduction

During the ~~Neoproterozoic (>635 million years ago)~~history of Earth, geological evidences support the formation of persistent ~~sea-ice~~ sea ice within the tropical regions, referred to as snowball Earth states (e.g. Hoffman et al., 2017). Because ice is highly reflective, the positive surface albedo feedback strengthens and exceeds the sum of other feedbacks while the Earth cools down.

The evolution of climate feedbacks as a function of temperature is referred ~~as state-dependency~~to as temperature-dependency. Whilst climate models agree that the surface albedo feedback increases in cold climates (e.g. Budyko, 1969), other climate feedbacks such as clouds are less understood in the context of cooling~~(e. g. Braun et al., 2022).~~

~~State-dependency~~ (e.g. Braun et al., 2022). Temperature-dependency in climate feedbacks has often been studied in warming climates~~(e. g. Caballero and Huber, 2013; Jonko et al. , 2013; Meraner et al. , 2013) , but rarely in cold climates (e. g. Colman and McAvaney, 2009).~~ (e.g. Caballero and Huber, 2013; Jonko et al., 2013; Meraner et al., 2013), but rarely in cold climates (e.g. Colman and McAvaney, 2009).

Pierrehumbert et al. (2011) proposed the Snowball Earth modelling intercomparisong project, or SnowMIP, as to compare modelling efforts within the field. SnowMIP was made of three atmosphere-ocean models, where two of them are older versions of the models applied in the current study (ECHAM5/MPIOM and CAM). SnowMIP paved the way to identifying the importance of circulation and clouds in snowball Earth initiation across models. Following SnowMIP, the importance of snow-albedo feedbacks and their relation to sea-ice albedo feedback was identified, as well as the interaction of ocean and atmosphere circulations (Voigt and Abbot, 2012). Due to the complexity of running a model into snowball Earth state, and the increasing cost of running higher-end models, there is to this day only a small number of published snowball Earth simulations and even less feedback analyses. To our knowledge, there is also no study that relates the snowball Earth transition and climate sensitivity.

The community definition of equilibrium climate sensitivity (ECS) is the long term global mean surface warming in response to a doubling of CO_2 over pre-industrial levels, excluding slow changes in ice sheets (Forster et al., 2021). ECS is perhaps the most important geophysical property for determining future global warming (Grose et al., 2018), and has long been the subject of investigation (Arrhenius, 1896). Currently, multiple lines of evidence are used in combination to constrain ECS, including a process based approach wherein individual feedbacks and forcing are constrained, use of the instrumental temperature record warming, and by interpreting estimates of temperature and forcing in various paleoclimates (Sherwood et al., 2020). The result is a substantially reduced uncertainty relative to earlier mainly climate model based assessments (Forster et al., 2021).

In this study, we quantify cloud feedbacks as the Earth ~~transits~~ transitions towards a snowball Earth state from pre-industrial conditions under low ~~CO2~~ CO_2 concentration. In particular, we focus on the contribution of cloud feedbacks over tropical oceans, as well as the interaction between cloud and sea-ice albedo feedbacks. Our motivation to investigate climate feedbacks in the snowball Earth transition stems from the fact that a number of models of the paleoclimate modelling intercomparison project phase 4 (PMIP4) fail to simulate the Last Glacial Maximum (LGM), a cold period with large ice sheets 21 000 years ago~~(e.g. Kageyama et al., 2021),~~ (e.g. Kageyama et al., 2021), despite being able to simulate warm paleoclimates (e.g. Pliocene, 3.2 million years ago~~(Haywood et al., 2020),~~ (Haywood et al., 2020), Eocene, 50 million years ago~~(Lunt et al., 2021))~~ (Lunt et al., 2021)). These climate models ~~start transiting to a snowball state at temperatures~~ simulate temperatures for the LGM substantially cooler than indicated by ~~LGM reconstructions(e.g. Zhu et al., 2021a)~~reconstructions, and show hints of runaway behaviour (e.g. Zhu and Poulsen, 2021b). Since they have strong positive cloud feedbacks they consequently exhibit high climate sensitivities~~, which is the long term temperature change after an abrupt doubling of atmospheric CO2 from pre-industrial concentrations~~. It could therefore be possible to use the models simulating stable LGM states by evaluating the

Table 1. Summary of the runs performed for this study. PI = Pre-industrial, LGM = Last Glacial Maximum. Solar constant is expressed in percentage of pre-industrial solar constant (1361 Wm^{-2}). *The runs started from an equilibrium state and ran for 100 years. **The runs were manually stopped and are expected to reach equilibrium in a cold non-snowball state.

Run	Length (years	Solar constant (%)	CO_2 (ppm)	Boundaries	Comments
Pre-industrial	*	100	284.32	PI	MPI-ESM1.2-CR
LGM	*	100	190	LGM	MPI-ESM1.2-LR
2xCO2	150	100	568.64	PI	MPI-ESM1.2-CR
abrupt50ppm	1156**	100	50	PI	MPI-ESM1.2-CR
1/8xCO2	1142	100	35.54	PI	MPI-ESM1.2-CR
1/16xCO2	639	100	17.80	PI	MPI-ESM1.2-CR
1/32xCO2	442	100	8.90	PI	MPI-ESM1.2-CR
1/64xCO2	338	100	4.45	PI	MPI-ESM1.2-CR
1/128xCO2	280	100	2.22	PI	MPI-ESM1.2-CR
1/256xCO2	245	100	1.11	PI	MPI-ESM1.2-CR
1/512xCO2	219	100	0.56	PI	MPI-ESM1.2-CR
1/1024xCO2	230	100	0.28	PI	MPI-ESM1.2-CR
1/2048xCO2	194	100	0.14	PI	MPI-ESM1.2-CR
1/128xCO2-fixalb	1046**	100	2.22	PI	locked albedo feedback
1/128xCO2-fixq	632**	100	2.22	PI	locked water vapor feedback
1/128xCO2-fixcld	946	100	2.22	PI	locked cloud feedback
1/512xCO2-fixcld	518	100	0.56	PI	locked cloud feedback
1/256xCO2-fixcld	648	100	1.11	PI	locked cloud feedback
1/64xCO2-fixcld	1453**	100	4.45	PI	locked cloud feedback
1/32xCO2-fixcld	1312**	100	8.90	PI	locked cloud feedback
lgm-S94	290	94	190	LGM	MPI-ESM1.2-LR
lgm-S93	198	93	190	LGM	MPI-ESM1.2-LR
lgm-S92	179	92	190	LGM	MPI-ESM1.2-LR
lgm-S91	148	91	190	LGM	MPI-ESM1.2-LR
lgm-S89	113	89	190	LGM	MPI-ESM1.2-LR
lgm-S85	75	85	190	LGM	MPI-ESM1.2-LR
S92-LR	179	92	284.32	PI	MPI-ESM1.2-LR
S85-LR	166	85	284.32	PI	MPI-ESM1.2-LR
CESM1.2	210	100	2.22	PI	CESM1.2

relationship between simulated LGM temperatures and the ECS of those models as to provide an ~~independent~~ upper limit constraint on climate sensitivity ~~by estimating~~ independent from previous estimates by calculating the temperature at which the Earth transits towards an unstable snowball Earth state. The constraint is essentially based on the fact that during the recent glacial cycles we have evidently not entered the snowball state.

To approach this problem with other climate models, we conclude our study with a short and easy-to-replicate experimental design of modern snowball Earth simulations. The results of this experiment are relevant for both climate sensitivity, as shown in this paper, as well as understanding the challenges around setting up the LGM simulation, a notoriously difficult ~~paleoclimate to model~~climate to simulate.

2 Methods

We use the Max Planck Institute for Meteorology Earth system model version 1.2, MPI-ESM1.2~~(Mauritsen et al., 2019)~~ (Mauritsen et al., 2019) to simulate snowball Earth transitions from pre-industrial (PI) and LGM initial conditions. The sea-ice and snow-albedo parametrisation is similar as other snowball Earth studies using an older version of this model (Voigt et al., 2011; Voigt and , except for the addition of meltponds which are described by Mauritsen et al. (2019). We perform abrupt and sustained changes of atmospheric ~~CO2~~ CO_2 concentrations or solar constant from the equilibrium states of PI or LGM. ~~Continents, non- CO2~~ The CO_2 concentrations are chosen as one half of the previous concentration, as CO_2 has a quasi-logarithmic forcing behaviour, and as to facilitate comparisons with other studies which uses doubling and halving, such as the ones of the non-linear modelling intercomparison project (nonlinMIP). Continents, non-CO_2 greenhouse gases and orbital configurations are kept as in PI or LGM. PI simulations use the coarse resolution ~~MPI- ESM1~~MPI-ESM1.2-CR (T31 spectral truncation, 31 atmospheric levels), which is faster and numerically more stable to extreme forcing. LGM boundary conditions are only available in the low resolution MPI-ESM1.2-LR (T63, 47 atmospheric levels). Radiative differences between the two models are small, and the climate sensitivity of MPI-ESM1.2-CR is slightly higher. While we do not expect ~~state-dependency~~ temperature-dependency to vary much across models, individual feedbacks are likely to slightly differ so we also initiate a few simulations from PI with MPI-ESM1.2-LR. Details of all simulations are summarised in Table~~1.~~ 1.

The growth of thick ~~sea-ice~~ sea ice leads to numerical instabilities in the model (~~>~~ > 12 meters). We do not artificially limit sea-ice growth as in other studies~~(Voigt and Marotzke, 2010; Voigt et al., 2011; Voigt and Abbot, 2012),~~ (Voigt and Marotzke, 2010; Voigt e , as it generates latent heat at the base of ~~sea-ice (Marotzke and Botzet, 2007)~~ sea ice (Marotzke and Botzet, 2007) which changes the required ~~CO2~~ CO_2 forcing for snowball Earth initiation~~(Hörner et al. , 2022~~ (Hörner et al., 2022). This results in all our simulations reaching numerical instability at some point when approaching a complete snowball Earth state due to the sea ice being too thick in narrow basins, such as the Baltic Sea. This does not affect our results, as we evaluate the transition in temperatures much higher than the one reached near the instability. Only the abrupt50ppm simulation was manually stopped as it is expected to reach an equilibrium in a cold non-snowball state (see Table 1 for details on run length).

2.1 Temperature and imbalance evolution of the simulations

We analyse the evolution of our simulations by studying how the TOA energetic imbalance changes with surface temperature. This approach is shown in Fig. 4 and Fig. 6 and has been first developed by Gregory et al. (2004). Here, each point of data is a one-year global average of the transient simulation as it responds to an initial forcing. Because the total feedback is at first negative, the system will attempt to reduce the TOA imbalance when exposed to positive or negative forcing. Consequently, in the case of an initial negative forcing, it cools down the climate. Therefore, the beginning of the simulation is where the temperature difference to PI is the closest to zero, and the imbalance is almost equal to the forcing imposed. The end of the simulation is the left-most point, when the temperature anomaly to PI is the largest.

In the real climate system, the climate would slowly cool down as the forcing from the Sun or greenhouse gases change only slowly. This comparison between slower transitions and our abruptly forced simulations is illustrated in Fig. 1. When a

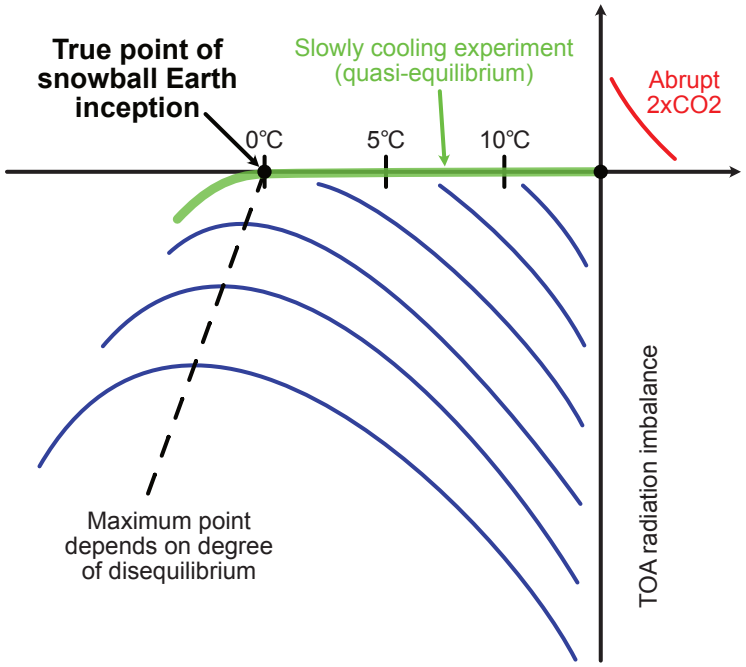

Figure 1. Schematic of TOA imbalance versus surface temperature difference to PI, as developed by Gregory et al. (2004). Here, we compare the behavior of our abrupt forcing simulations, as they cool down, to the behavior of a real world transition wherein CO_2 is slowly and gradually reduced (green line).

negative forcing is slowly applied, for instance if CO_2 was slowly decreasing over time, the climate system would maintain a quasi-equilibrium and move along the green line to colder temperatures, until the true instability leading to a snowball Earth state is met. In our simulations, the point the closest to equilibrium, i.e. the least negative TOA imbalance, serves as the inception value. If a simulation was to be brought to higher CO_2 concentration, it is at this point that the equilibrium would be reached first. Because the simulations miss this equilibrium point, they will not reach any other equilibrium until a new climate state, most likely the snowball Earth state, is found, since any other year is further out of balance than the year at this equilibrium point. Therefore, we can define the inception temperature towards snowball Earth as the temperature of the year with the least negative TOA imbalance. By definition it is also the year where the tangential, which is the total climate feedback, would be strictly zero, as it becomes positive after, at lower temperatures.

Unfortunately, as we shall see, the simulated point slightly differs from the true inception point due to time-dependent effects proportional to the degree of disequilibrium. It appears that when the forcing is strongly negative, the inception point in the Gregory analysis shifts to lower temperatures. We speculate that this is a kind of time-dependent feedback effect whereby the positive feedback from formation of sea ice is delayed by the large thermal inertia of the oceans. Therefore, to estimate a

model's true snowball Earth inception point it is necessary to carry out multiple abrupt forcing experiments as is done in this study.

2.2 Climate feedback calculations

Climate feedbacks are diagnosed using the partial radiative perturbation (PRP) method~~(Wetherald and Manabe, 1988; Colman and McAvaney, 1997)~~ (Wetherald and Manabe, 1988; Colman and McAvaney, 1997). Details of its online implementation in MPI-ESM1.2 are in~~Meraner et al. (2013).~~ Meraner et al. (2013). The PRP method calculates individual contributions of surface albedo, clouds, temperature and water vapor changes to top-of-atmosphere fluxes, by exchanging related variables between a control climate state and the transient state analysed. Because the length of each run varies with the forcing amplitude, we compute climate feedbacks by regressing the top-of-atmosphere radiation balance changes arising from albedo, clouds, temperature, water vapor changes over bins of data points spanning a global temperature ranges of 5°C. We apply the same method in the maps of Fig. 3, whereby the temperature indicated is the middle point of the temperature range.

We furthermore perform runs where we separately lock surface albedo, clouds or water vapor in the radiation calculations to the control state, i.e. the corresponding feedbacks do not contribute to the radiation balance. The implementation in MPI-ESM1.2 is described in~~Mauritsen et al. (2013).~~ Mauritsen et al. (2013). These locked-feedback transient simulations read the pre-industrial control albedo, clouds, temperature and humidity and impose them on the radiation parameterization regardless of the changes the system is experiencing, such as the increasing extent of ~~sea-ice~~sea ice.

2.3 Constraint on Earth's climate sensitivity

The relationship between LGM simulated temperatures and the climate sensitivity of models have been used in emergent constraint framework to infer the Earth~~'~~'s true climate sensitivity owing to geological reconstructions of LGM temperatures~~(Hargreaves et al. , 2012; Schmidt et al., 2014; Renoult et al., 2020, 2023).~~ (Hargreaves et al., 2012; Schmidt et al., 2014; Renoult et al., 2020, 2 . The novel constraint on Earth~~'~~'s climate sensitivity developed here uses the same relationship, where the regression parameters are calculated via ordinary least squares method~~, but we replace the geological reconstruction of the LGM by the temperature at which the Earth transits to a snowball Earth~~. This constraint relies on the simple fact that the LGM was a stable glacial climate ~~, and therefore the highest value of Earth'~~and did not transition to a snowball state. Therefore, Earth's climate sensitivity ~~before the LGM enters~~ could not have been higher than the point at which the planet would transition into a snowball state ~~represents the upper limit on climate sensitivity~~before the LGM. As such, the presented constraint provides a physical upper bound on ECS, not a best estimate.

Recently,~~Renoult et al. (2023)~~ Renoult et al. (2023) showed that structural uncertainties and ~~state-dependencies~~ temperature-dependenci in climate feedbacks hinder the relationship between LGM temperature and climate sensitivity, which is computed from warm simulations (4 times pre-industrial ~~CO2 (Gregory et al., 2004)). We minimize~~ CO_2 (Gregory et al., 2004)). The authors minimized the issue by adding to the PMIP4 ensemble an ensemble of CESM models (CESM1.2, CESM1.3 and CESM2.1)~~in a similar way as described by Renoult et al. (2023). Besides increasing the size of the PMIP4 ensemble, single-model ensembles~~

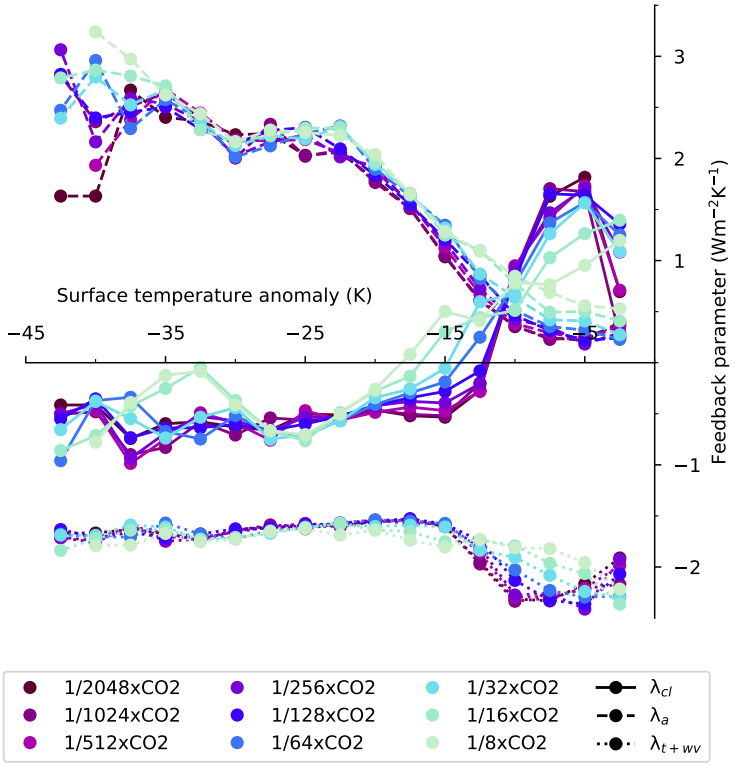

Figure 2. Evolution of the climate feedback parameters of clouds (λ_{cl}), albedo (λ_a) and temperature and water vapor combined (λ_{t+wv}) with global surface temperature anomaly compared to pre-industrial (K) under all CO_2 forcing.

~~(or in this case, single-family models) have reduced structural uncertainties, in particular regarding ice sheet forcing, albeit they could add statistical dependency issues within the relationship~~. ~~Here we assume the three CESM models are sufficiently different to avoid this issue~~However, the relationship is similar whether CESM2.1 is included or not, which implies that the lower-ECS CESM models are not necessary to preserve the quality of the relationship. We decide therefore to not include them, mainly because we only have access to their sea-surface temperature data whereas our analyses are mostly based on surface temperatures including land.

3 Analysis of surface albedo and cloud feedbacks

We perform experiments with abrupt decreases of ~~CO2~~ CO_2 concentrations ranging from 1/8 to 1/2048 of pre-industrial ~~CO2~~ CO_2 concentration using the MPI-ESM1.2-CR model to simulate snowball Earth inception and breakdown climate feedbacks (Section~~2~~ 2). For clarity, we report global mean surface temperature anomalies to pre-industrial in units of K, and global mean surface absolute temperatures in °C. The strengthening surface albedo feedback has often been considered the main

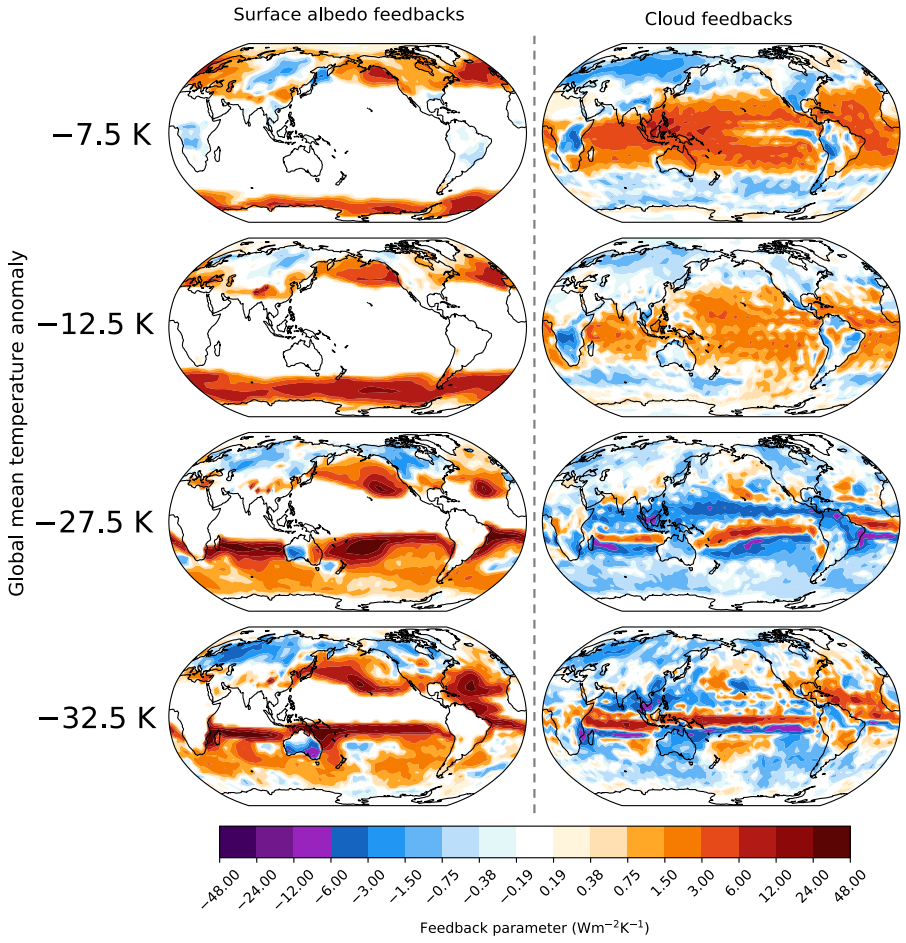

Figure 3. Maps of the surface albedo (left column) and cloud (right column) feedbacks at four average global temperatures in the 1/16xCO2 simulation. The global mean temperature anomaly indicated is the middle point of the temperature range over which the feedbacks are computed, taking bins of 5 degrees of cooling.

driver in the snowball Earth instability, yet positive cloud feedbacks exceed the surface albedo feedback during the initial 10 K of cooling (Fig.~~1~~ 2). This strengthening arises from positive tropical cloud feedbacks (Fig.~~2~~ 3) due to an increase in shallow cloud coverage over the tropical oceans (Appendix Fig.~~B1). Below -~~ B1). Cloud feedbacks are increasingly more positive as the initial forcing is increasingly stronger, which amplify tropical cooling. Below −~~20 K relative to pre-industrial, cloud feedbacks switch sign and are globally negative and weaker than the surface albedo feedback, although there still exists strong positive cloud feedbacks ahead of the advancing sea-ice edge in both hemispheres (Fig.~~2~~ 3). Indeed, because the sea-ice surface is cold, clouds are preferentially over open water which is warmer and a source of moisture ~~(e.g. Wall et al., 2017),~~ (e.g. Wall et al., 2017), where they facilitate further cooling of the ocean. All in all, cloud feedbacks substantially contribute

to early cooling in response to reduced ~~CO2~~CO_2. During the transition, the positive surface albedo feedback exceeds the combined cloud, temperature and water vapor feedbacks at temperatures between ~~-~~15 K and ~~-~~20 K below pre-industrial (Fig.~~3~~ 4). This leads to a global instability and is concomitant with the acceleration of ~~southern~~ the equatorward sea-ice edge into the sub-tropics, resulting in strong global cooling towards the snowball state.

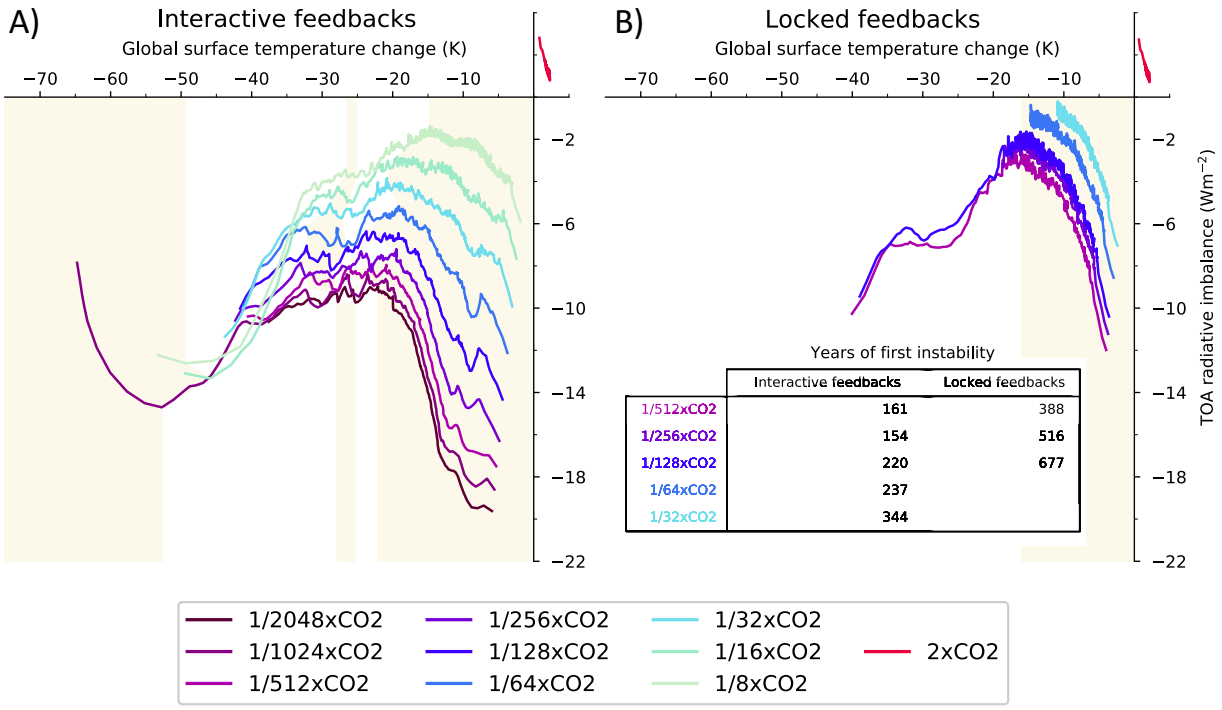

Figure 4. A) Top-of-atmosphere radiative imbalance (Wm^{-2}) versus global surface temperature anomaly with pre-industrial conditions (K) under varying CO_2 forcing and B) same but with cloud feedbacks locked to that of the control state. A run with an abrupt doubling of CO_2 (2xCO2) is shown for comparison. Colored phases correspond to negative feedback, white phases positive feedback. The years of the first instability between interactive and locked feedbacks are annotated.

The diagnostics presented above is suggestive that cloud feedback may be an important climate driver towards the ~~snow ball~~ snowball transition. To demonstrate that this is indeed the case, we isolate the importance of each feedback using the feedback locking technique (Section~~2~~ 2) on various simulations, where each feedback mechanism is disabled one after the other (Fig.~~3-B~~ 4-B). When the cloud feedback is locked, the instability is reached at a similar global mean temperature as in the non-locked simulations, between ~~-~~15 K and ~~-~~20 K (Fig.~~3-A~~ 4-A). However, cloud feedback locking drastically increases the forcing required to initiate the snowball Earth inception, and considerably slow down the transition to snowball Earth. We find that simulations at ~~CO2~~ CO_2 concentration of 1/64 times pre-industrial levels and lower are required to trigger the transition with locked cloud feedbacks, which is a factor ten less than the concentration required with interactive cloud

feedbacks. The surface albedo-locked simulation does not reach a snowball instability as it enters quasi-equilibrium below the transition temperature of around ~~–~~15 K. Similarly, the simulation reaches a quasi-equilibrium below ~~–~~10 K when the water vapor feedback is locked (Appendix Fig.~~B2~~ B2). The water vapor feedback actually does not strengthen with cooling so is not itself the cause of the snowball instability, however its large positive feedback is important for allowing the surface albedo to trigger the instability.

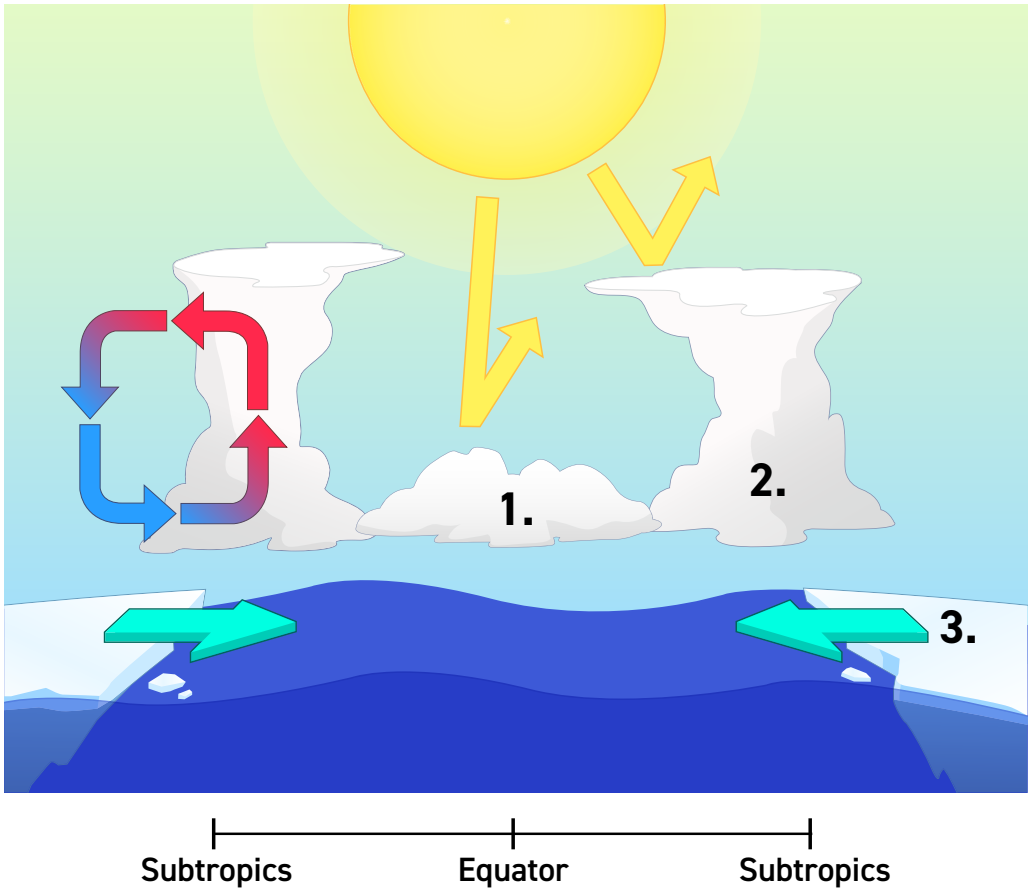

Figure 5. Contribution of cloud feedbacks to ocean cooling and interaction with sea ice. 1. Tropical surface cooling by positive low-level cloud feedback. 2. Sea surface cooling ahead of ice edge. 3. Faster sea-ice advance, facilitated by winds pushing sea ice equatorwards (Appendix Fig. B3).

Thus, the role of cloud feedback is different from that of the surface albedo feedback: 1) positive cloud feedbacks facilitate an early tropical cooling, and this effect is increased with increasing forcing, 2) positive cloud feedbacks ahead of the advancing

sea-ice edge and its effect on tropical oceans accelerate the transition to snowball Earth and decrease the temperature of instability, as summarized in Fig.~~4~~ 5; 3) cloud feedbacks substantially increase the threshold ~~CO2~~ CO_2 level required for snowball Earth initiation and 4) the entry of ~~sea-ice~~ sea ice into the southern subtropics results in the surface albedo feedback exceeding the sum of the negative feedbacks. Whereas the albedo feedback is responsible for the transition and the main driver to the complete glaciation, our results emphasise an important contribution of cloud feedbacks. And as it happens, cloud feedbacks are also the main cause of inter model spread in climate sensitivity~~(e.g. Zelinka et al., 2020),~~ (e.g. Zelinka et al., 2020), a fact which we shall exploit in Section~~5.~~ 5.

4 Model evidence for the snowball transition temperature

The temperature at which the climate transits towards a snowball Earth state is broadly similar across the different ~~CO2~~ CO_2 forcing experiments (Fig.~~3~~ 4), as well as whether the experiment is initialized from a PI or an LGM state, as shown in Appendix~~A~~ A, which demonstrates the importance of background temperature control over the climate feedbacks which drive the transition. In particular, sea-ice formation is primarily temperature-dependent, and the amplitude of the sea-ice albedo feedback is practically independent of the strength of the negative forcing (Fig.~~1~~ 2). We can expect such ~~state-dependency~~ temperature-dependency to be similar across climate models, which would contribute to them having a similar temperature of entering the snowball transition. Similarly, the winds pushing ~~sea-ice~~ sea ice equatorwards (Appendix Fig.~~B3~~ B3), in connection with temperature contrast between ~~sea-ice~~ sea ice and open ocean, and which are concomitant with positive cloud feedbacks ahead of sea-ice edge are also expected to behave in similar ways across models since they broadly simulate the same circulation. A simple geometric argument for a transition temperature close to 0°C is that it happens when the ice edge enters the sub-tropics at about 30 degrees latitude, leaving about half the Earth still ice free and hence above the freezing temperature, and the other half at temperatures below. When abruptly decreasing the ~~CO2~~ CO_2 concentration to 50 ppm (around 1/4 of pre-industrial ~~CO2~~CO_2), we find hints of instability near the global mean temperature of 0°C (~~-~~near −15 K relative to pre-industrial), but the model seems to be stable for 1848 years until it crashes due to thick ~~sea-ice (Section2~~sea ice (Section 2). This indicates that it is unlikely that the inception temperature happens at a temperature substantially warmer than 0°C.

Nevertheless, the transition temperatures of each phase show a slight shift to lower values under stronger negative forcing. ~~130~~ Therefore, the climate system deviates from pure ~~state-dependent~~ temperature-dependent behaviour as the strength of the radiative cooling and the speed of transition to snowball Earth increases. These time-dependency effects have often been described in the literature following extreme cooling rates~~(Bendtsen and Bjerrum, 2002; Marotzke and Botzet, 2007), and~~ (Bendtsen and Bjerrum, 2002; Marotzke and Botzet, 2007), and we believe to be due to the large heat capacity of the ocean, as well as differences in ocean mixed layer depths and direct ~~CO2~~ CO_2 forcing across different regions: in certain circumstances, this can result in local temperatures dropping faster than global temperatures (Appendix Fig.~~B4-A~~ B4-A), and hence out of sync with the sea-ice extent controlling the surface albedo feedback. Ocean convective mixing is also increasingly more efficient at evacuating heat for larger surface cooling, indicated by an increasing peak of the strength of the Atlantic meridional overturning circulation (AMOC) in Appendix Fig.~~B4-B~~ B4-B. The associated ocean currents on the contrary drag ~~sea-ice~~ sea ice polewards

and can slow down the sea-ice edge advance~~(Voigt and Abbot, 2012)~~ (Voigt and Abbot, 2012). All in all, we suggest slow, low forcing simulations are preferable when analysing snowball Earth transitions, as 1) fast transitions to snowball Earth are hardly realistic, as geological snowball states may form over millions of years~~(e.g. Schrag et al., 2002)~~ (e.g. Schrag et al., 2002)
215 and 2) fast transitions ~~involves~~ involve temporal effects which would depart from ~~state-dependency~~temperature-dependency. All together, these considerations support the higher transition temperature close to 0°C found in the experiments with weak forcing.

5 Motivation for simulations and potential constraint on climate sensitivity

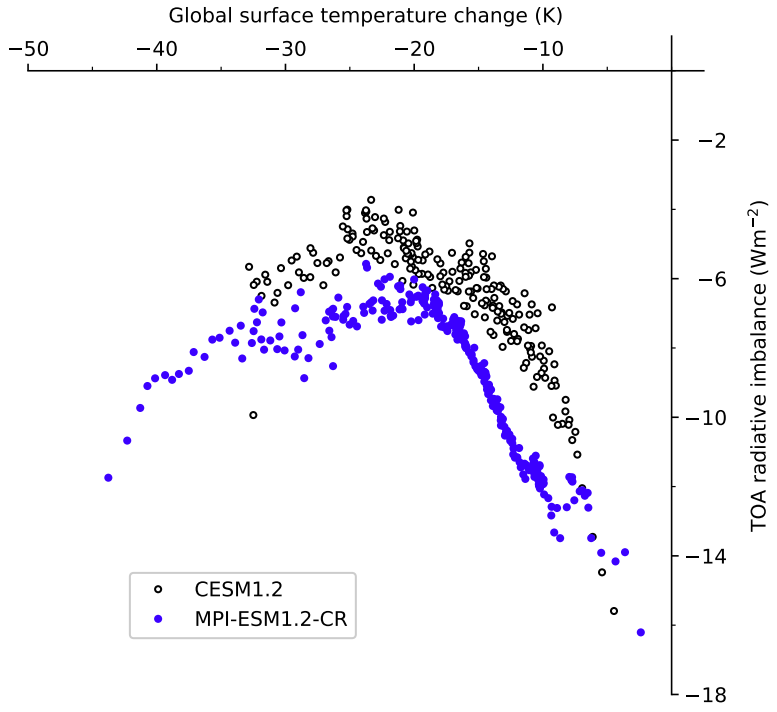

Figure 6. Top-of-atmosphere radiative imbalance (Wm^{-2}) versus global surface temperature anomaly with pre-industrial conditions (K) in abrupt 1/128xCO2 simulations with the models MPI-ESM1.2-CR and CESM1.2.

While we expect the ~~state-dependency~~ temperature-dependency to behave similarly across models, it is currently not known
220 whether the temperature threshold of 0°C that we find in MPI-ESM1.2-CR is indeed universal. The CESM model family has ~~notoriously~~ performed several snowball Earth simulations~~(Yang et al., 2012b, a; Eisenman and Armour, 2024), and~~ (Yang et al., 2012b, a; Eisenman and Armour, 2024), and while the model CESM2 also transits towards a snowball Earth around 0°C under similar ~~CO2 forcing(Eisenman and Armour, 2024),~~ CO_2 forcing (Eisenman and Armour, 2024), models

such as CCSM3 and CCSM4 can have stable waterbelt states with abrupt but smaller transitions. To further test this, we perform an abrupt 1/128xCO2 simulation with the model CESM1.2. CESM1.2 has been used for several deep-time simulations~~(Li et al., 2022),~~ (Li et al., 2022), but to our knowledge never for snowball Earth states. CESM1.2 shows a similar instability ~~than~~ as MPI-ESM1.2, which at 1/128xCO2 is around a temperature of ~~0°C,~~ -24 K, but considering the time-dependency effects discussed in this study (Fig.~~5).~~ 6). Therefore we would expect for CESM1.2 the transition to happen close to 0°C in a slowly cooling simulation under a lower forcing, as was the case for MPI-ESM1.2.

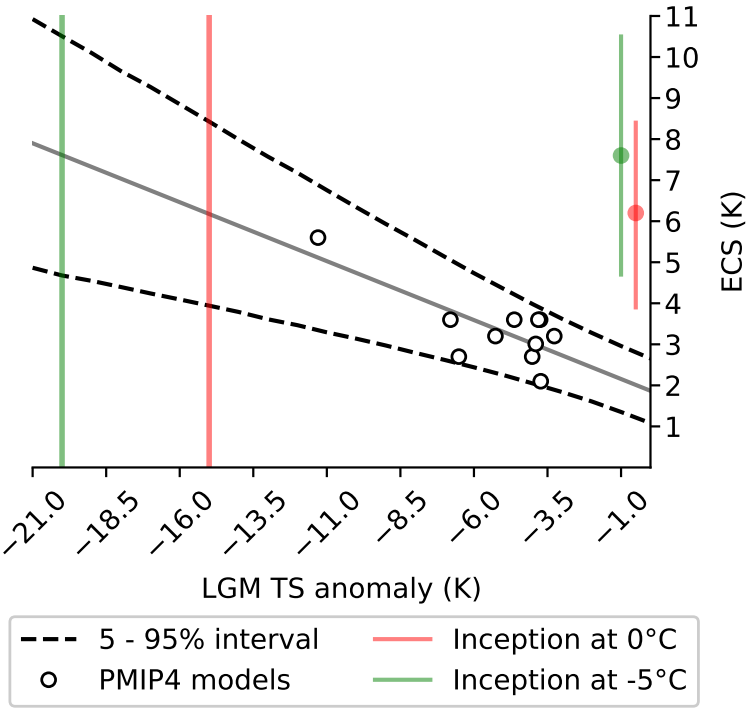

Figure 7. Relationship between modelled LGM surface temperature anomaly relative to pre-industrial and the climate sensitivity of PMIP4 models. The upper bound on climate sensitivity can be constrained using the temperature at which the climate starts transiting to snowball Earth, which is around -15 K global mean surface temperature anomaly (red). As a comparison, we calculate the upper bound if the transition was instead at -20 K (green).

There is an ongoing discussion on whether climate models with large cloud feedbacks and consequently high climate sensitivity are compatible with the LGM~~(Zhu et al., 2022; Burls and Sagoo, 2022).~~ (Zhu et al., 2022; Burls and Sagoo, 2022). Models with high sensitivity simulate LGM temperatures around the snowball Earth inception temperature of around 0°C and are usually unstable. This in fact is to be expected if the inception temperature is controlled by the temperature-dependent behaviour of the climate feedbacks, where the threshold before transiting to a snowball Earth state would be similar across models. Variations of that threshold could be due to for example different parameterizations of sea-ice albedo~~, tropical shallow~~

~~clouds~~. In the case of tropical shallow cloud feedbacks, despite considerably increasing the sensitivity of the climate to enter snowball Earth, ~~these feedbacks~~ they do not seem to ~~modify the~~ affect the snowball Earth inception temperature (Fig.~~3~~ 4).

It is therefore possible to derive the upper limit of climate sensitivity from the models with stable LGM states (Section~~2~~ 2), using as snowball temperature threshold a global mean temperature close to 0°C, since both LGM and PI states transit towards a snowball Earth state at similar temperatures (Appendix Fig.~~A1~~ A1). In this way, we find that it is implausible that climate sensitivity exceeds ~~5.5 K (4.4 – 6.6~~6.2 K (3.9 – 8.4, 90% confidence interval, Fig.~~6~~ 7). This upper limit is close to the sensitivity of CESM2 (5.6 K), which simulates an LGM temperature anomaly of ~~–~~ 11.3 K~~(-7.0 K in SSTs) (Zhu et al., 2021b), (Zhu et al., 2021),~~ just above the global mean temperature of 0°C. Additional support for this limit is obtained from a slightly more sensitive version of the model which is unstable when run with LGM boundary conditions~~(Zhu et al.~~ (Zhu et al., 2022).

Because there is an uncertainty on whether the inception temperature would be close to 0°C across models, we test the sensitivity of our constraint by applying a large uncertainty decreasing it to -5°C (Fig. 7. In this case, we find that the upper bound on ECS cannot exceed 7.6 K (4.7 – 10.5, ~~2022).~~ 90% confidence interval). This is a relatively modest change of 1.4 K in the upper bound, considering the large change in inception temperature . The uncertainty on the inception therefore has a small influence on the upper bound on ECS estimate, and the value obtained here is in agreement with estimates from other lines of evidence, or in many cases even a stronger constraint (Forster et al., 2021).

This ~~approach~~ here proposed approach to provide an upper bound on climate sensitivity could have a great potential, in particular as independent constraints from paleoclimates are ~~increasingly useful (Sherwood et al. , 2020).~~ found to be increasingly useful (Sherwood et al., 2020). Nevertheless, to support ~~this constraint requires an effort from~~ the constraint it would be beneficial that several modelling centres to both publish their LGM simulations, even if they fail to stabilise, and narrow down the uncertainty on the instability threshold. It is important to know whether many models have a threshold gravitating around 0°C, similarly to MPI-ESM1.2-CR, MPI-ESM1.2-LR and CESM1.2.

To tackle this problem, we offer the following experimental design, which is short and easy-to-replicate:

1. Run a pre-industrial state, with the ~~CO2~~ CO_2 concentration set to 1/128 times the PI value, until the model reaches at least the initial instability leading to the snowball Earth state. The chosen ~~CO2~~ CO_2 concentration should be a fair trade off between a minimal simulation length and the time-dependency effects discussed in this study. If time allows, complement with less strong reductions to investigate the time-dependency.

2. Generate a plot of top-of-atmosphere radiation imbalance versus ~~surfce~~ surface temperature anomaly relative to PI, as in Fig.~~3.~~ 4. Report the instability threshold temperature, from surface and sea-surface temperature, as well as the global sea-ice concentration.

3. ~~For modelling centres simulating the LGM, we strongly suggest to publish runs which led to instabilities.~~

The results could support the novel constraint on climate sensitivity presented in this study, but also help understanding instabilities in LGM simulations, a paleoclimate notoriously difficult to model, in particular for higher climate sensitivity models. We advocate that multi-model comparisons of snowball Earth transitions, as well as single-model ensembles with

varying climate sensitivity, would better support the relationship between simulated LGM temperatures and the upper bound on model Earth''s climate sensitivity. The main strength of this constraint is that it is independent of paleoclimate reconstructions and simply relies on the fact that Earth did not undergo a transition to a snowball state 21 000 years ago, or during any earlier glacial cycles during the Pleistocene, providing a valuable additional line of evidence to those already used in the community~~(Sherwood et al. , 2020; Forster et al., 2021).~~ (Sherwood et al., 2020; Forster et al., 2021).

Data availability. The outputs of the simulations shown in this study can be downloaded from https://doi.org/10.5281/zenodo.8117483

Author contributions. The idea of the study was conceived by MR. MR performed all simulations, analyses and figures. The paper was written by MR, JH, NS and TM.

Competing interests. The authors declare that they have no conflict of interest.

Acknowledgements. We thank Christoph Braun, Aiko Voigt and Raymond Pierrehumbert for the scientific discussions which helped advancing this study. We thank Eduardo Carril for designing Figure 5. The computations and data storage were enabled by resources provided by the National Academic Infrastructure for Supercomputing in Sweden (NAISS) and the Swedish National Infrastructure for Computing (SNIC) at the National Supercomputer Centre at Linköping University, partially funded by the Swedish Research Council through grant agreements no. 2022-06725 and no. 2018-05973. This research has been supported by the European Research Council, H2020 European Research Council (highECS (770765) and CONSTRAIN (820829)).

References

Arrhenius, S.: On the Influence of Carbonic Acid in the Air upon the Temperature of the Ground, Philosophical Magazine and Journal of Science, 41, 237–276, 1896.

Bendtsen, J. and Bjerrum, C. J.: Vulnerability of climate on Earth to sudden changes in insolation, Geophysical Research Letters, 29, 1–1, 2002.

Braun, C., Hörner, J., Voigt, A., and Pinto, J. G.: Ice-free tropical waterbelt for Snowball Earth events questioned by uncertain clouds, Nature Geoscience, pp. 1–5, 2022.

Budyko, M. I.: The effect of solar radiation variations on the climate of the Earth, tellus, 21, 611–619, 1969.

Burls, N. and Sagoo, N.: Increasingly sophisticated climate models need the out-of-sample tests paleoclimates provide, Journal of Advances in Modeling Earth Systems, p. e2022MS003389, 2022.

Caballero, R. and Huber, M.: State-dependent climate sensitivity in past warm climates and its implications for future climate projections, Proceedings of the National Academy of Sciences, 110, 14 162–14 167, 2013.

Colman, R. and McAvaney, B.: A study of general circulation model climate feedbacks determined from perturbed sea surface temperature experiments, Journal of Geophysical Research: Atmospheres, 102, 19 383–19 402, https://doi.org/10.1029/97JD00206, 1997.

Colman, R. and McAvaney, B.: Climate feedbacks under a very broad range of forcing, Geophysical Research Letters, 36, https://doi.org/10.1029/2008GL036268, 2009.

Eisenman, I. and Armour, K. C.: The radiative feedback continuum from Snowball Earth to an ice-free hothouse, Nature Communications, 15, 6582, 2024.

Forster, P., Storelvmo, T., Armour, K., Collins, W., Dufresne, J., Frame, D., Lunt, D., Mauritsen, T., Palmer, M., Watanabe, M., Wild, M., and Zhang, H.: The Earth's Energy Budget, Climate Feedbacks, and Climate Sensitivity, in: Climate Change 2021: The Physical Science Basis. Contribution of Working Group I to the Sixth Assessment Report of the Intergovernmental Panel on Climate Change, Cambridge University Press, 2021.

Gregory, J. M., Ingram, W., Palmer, M., Jones, G., Stott, P., Thorpe, R., Lowe, J., Johns, T., and Williams, K.: A new method for diagnosing radiative forcing and climate sensitivity, Geophysical Research Letters, 31, https://doi.org/10.1029/2003GL018747, 2004.

Grose, M. R., Gregory, J., Colman, R., and Andrews, T.: What Climate Sensitivity Index Is Most Useful for Projections?, Geophysical Research Letters, 45, 1559–1566, https://doi.org/https://doi.org/10.1002/2017GL075742, 2018.

Hargreaves, J. C., Annan, J. D., Yoshimori, M., and Abe-Ouchi, A.: Can the Last Glacial Maximum constrain climate sensitivity?, Geophysical Research Letters, 39, https://doi.org/10.1029/2012GL053872, 2012.

Haywood, A. M., Tindall, J. C., Dowsett, H. J., Dolan, A. M., Foley, K. M., Hunter, S. J., Hill, D. J., Chan, W.-L., Abe-Ouchi, A., Stepanek, C., et al.: The Pliocene Model Intercomparison Project Phase 2: large-scale climate features and climate sensitivity, Climate of the Past, 16, 2095–2123, 2020.

Hoffman, P. F., Abbot, D. S., Ashkenazy, Y., Benn, D. I., Brocks, J. J., Cohen, P. A., Cox, G. M., Creveling, J. R., Donnadieu, Y., Erwin, D. H., et al.: Snowball Earth climate dynamics and Cryogenian geology-geobiology, Science Advances, 3, e1600 983, 2017.

Hörner, J., Voigt, A., and Braun, C.: Snowball Earth initiation and the thermodynamics of sea ice, Journal of Advances in Modeling Earth Systems, p. e2021MS002734, 2022.

Jonko, A. K., Shell, K. M., Sanderson, B. M., and Danabasoglu, G.: Climate feedbacks in CCSM3 under changing CO 2 forcing. Part II: variation of climate feedbacks and sensitivity with forcing, Journal of Climate, 26, 2784–2795, 2013.

Kageyama, M., Harrison, S. P., Kapsch, M.-L., Lofverstrom, M., Lora, J. M., Mikolajewicz, U., Sherriff-Tadano, S., Vadsaria, T., Abe-Ouchi, A., Bouttes, N., Deepak, C., Gregoire, L. J., Ivanovic, R. F., Izumi, K., LeGrande, A. N., Lhardy, F., Lohmann, G., Morozova, P. A., Ohgaito, R., Paul, A., Peltier, W., Poulsen, C. J., Quiquet, A., Roche, D. M., Shi, X., Tierney, J. E., Valdes, P. J., Volodin, E., and Zhu, J.: The PMIP4 Last Glacial Maximum experiments: preliminary results and comparison with the PMIP3 simulations, Climate of the Past, 17, 1065–1089, https://doi.org/https://doi.org/10.5194/cp-17-1065-2021, 2021.

Li, X., Hu, Y., Guo, J., Lan, J., Lin, Q., Bao, X., Yuan, S., Wei, M., Li, Z., Man, K., et al.: A high-resolution climate simulation dataset for the past 540 million years, Scientific Data, 9, 371, 2022.

Lunt, D. J., Bragg, F., Chan, W.-L., Hutchinson, D. K., Ladant, J.-B., Morozova, P., Niezgodzki, I., Steinig, S., Zhang, Z., Zhu, J., Abe-Ouchi, A., Anagnostou, E., de Boer, A. M., Coxall, H. K., Donnadieu, Y., Foster, G., Inglis, G. N., Knorr, G., Langebroek, P. M., Lear, C. H., Lohmann, G., Poulsen, C. J., Sepulchre, P., Tierney, J. E., Valdes, P. J., Volodin, E. M., Dunkley Jones, T., Hollis, C. J., Huber, M., and Otto-Bliesner, B. L.: DeepMIP: model intercomparison of early Eocene climatic optimum (EECO) large-scale climate features and comparison with proxy data, Climate of the Past, 17, 203–227, https://doi.org/10.5194/cp-17-203-2021, 2021.

Marotzke, J. and Botzet, M.: Present-day and ice-covered equilibrium states in a comprehensive climate model, Geophysical Research Letters, 34, 2007.

Mauritsen, T., Graversen, R. G., Klocke, D., Langen, P. L., Stevens, B., and Tomassini, L.: Climate feedback efficiency and synergy, Climate Dynamics, 41, 2539–2554, 2013.

Mauritsen, T., Bader, J., Becker, T., Behrens, J., Bittner, M., Brokopf, R., Brovkin, V., Claussen, M., Crueger, T., Esch, M., Fast, I., Fiedler, S., Fläschner, D., Gayler, V., Giorgetta, M., Goll, D. S., Haak, H., Hagemann, S., Hedemann, C., Hohenegger, C., Ilyina, T., Jahns, T., Jimenéz-de-la Cuesta, D., Jungclaus, J., Kleinen, T., Kloster, S., Kracher, D., Kinne, S., Kleberg, D., Lasslop, G., Kornblueh, L., Marotzke, J., Matei, D., Meraner, K., Mikolajewicz, U., Modali, K., Möbis, B., Müller, W. A., Nabel, J. E. M. S., Nam, C. C. W., Notz, D., Nyawira, S.-S., Paulsen, H., Peters, K., Pincus, R., Pohlmann, H., Pongratz, J., Popp, M., Raddatz, T. J., Rast, S., Redler, R., Reick, C. H., Rohrschneider, T., Schemann, V., Schmidt, H., Schnur, R., Schulzweida, U., Six, K. D., Stein, L., Stemmler, I., Stevens, B., von Storch, J.-S., Tian, F., Voigt, A., Vrese, P., Wieners, K.-H., Wilkenskjeld, S., Winkler, A., and Roeckner, E.: Developments in the MPI-M Earth System Model version 1.2 (MPI-ESM1. 2) and Its Response to Increasing CO2, Journal of Advances in Modeling Earth Systems, 11, 998–1038, https://doi.org/10.1029/2018MS001400, 2019.

Meraner, K., Mauritsen, T., and Voigt, A.: Robust increase in equilibrium climate sensitivity under global warming, Geophysical Research Letters, 40, 5944–5948, https://doi.org/10.1002/2013GL058118, 2013.

Muglia, J. and Schmittner, A.: Glacial Atlantic overturning increased by wind stress in climate models, Geophysical Research Letters, 42, 9862–9868, https://doi.org/10.1002/2015GL064583, 2015.

Pierrehumbert, R., Abbot, D., Voigt, A., and Koll, D.: Climate of the Neoproterozoic, Annual Review of Earth and Planetary Sciences, 39, 417–460, 2011.

Renoult, M., Annan, J. D., Hargreaves, J. C., Sagoo, N., Flynn, C., Kapsch, M.-L., Li, Q., Lohmann, G., Mikolajewicz, U., Ohgaito, R., Shi, X., Zhang, Q., and Mauritsen, T.: A Bayesian framework for emergent constraints: case studies of climate sensitivity with PMIP, Climate of the Past, 16, 1715–1735, https://doi.org/10.5194/cp-16-1715-2020, 2020.

Renoult, M., Sagoo, N., Zhu, J., and Mauritsen, T.: Causes of the weak emergent constraint on climate sensitivity at the Last Glacial Maximum, Climate of the Past, 19, 323–356, https://doi.org/10.5194/cp-19-323-2023, 2023.

Schmidt, G., Annan, J., Bartlein, P., Cook, B., Guilyardi, É., Hargreaves, J., Harrison, S., Kageyama, M., LeGrande, A., Konecky, B., Lovejoy, S., Mann, M. E., Masson-Delmotte, V., Risi, C., Thompson, D., Timmermann, A., Tremblay, L.-B., and Yiou, P.: Using palaeo-climate comparisons to constrain future projections in CMIP5, Climate of the Past, 10, 221–250, https://doi.org/10.5194/cp-10-221-2014, 2014.

Schrag, D. P., Berner, R. A., Hoffman, P. F., and Halverson, G. P.: On the initiation of a snowball Earth, Geochemistry, Geophysics, Geosystems, 3, 1–21, 2002.

Sherriff-Tadano, S., Abe-Ouchi, A., Yoshimori, M., Oka, A., and Chan, W.-L.: Influence of glacial ice sheets on the Atlantic meridional overturning circulation through surface wind change, Climate dynamics, 50, 2881–2903, https://doi.org/10.1007/s00382-017-3780-0, 2018.

Sherwood, S., Webb, M., Annan, J., Armour, K., Forster, P., Hargreaves, J., Hegerl, G., Klein, S., Marvel, K., Rohling, E., Watanabe, M., Andrews, T., Braconnot, P., Bretherton, C., Foster, G., Hausfather, Z., von der Heydt, A., Knutti, R., Mauritsen, T., Norris, J., Proistosescu, C., Rugenstein, M., Schmidt, G., Tokarska, K., and Zelinka, M.: An assessment of Earth's climate sensitivity using multiple lines of evidence, Reviews of Geophysics, p. e2019RG000678, https://doi.org/10.1029/2019RG000678, 2020.

Voigt, A. and Abbot, D.: Sea-ice dynamics strongly promote Snowball Earth initiation and destabilize tropical sea-ice margins, Climate of the Past, 8, 2079–2092, 2012.

Voigt, A. and Marotzke, J.: The transition from the present-day climate to a modern Snowball Earth, Climate dynamics, 35, 887–905, 2010.

Voigt, A., Abbot, D. S., Pierrehumbert, R. T., and Marotzke, J.: Initiation of a Marinoan Snowball Earth in a state-of-the-art atmosphere-ocean general circulation model, Climate of the Past, 7, 249–263, 2011.

Wall, C. J., Kohyama, T., and Hartmann, D. L.: Low-cloud, boundary layer, and sea ice interactions over the Southern Ocean during winter, Journal of Climate, 30, 4857–4871, 2017.

Wetherald, R. and Manabe, S.: Cloud feedback processes in a general circulation model, Journal of Atmospheric Sciences, 45, 1397–1416, https://doi.org/10.1175/1520-0469(1988)045<3C1397:CFPIAG>3E2.0.CO;2, 1988.

Yang, J., Peltier, W., and Hu, Y.: The initiation of modern soft and hard Snowball Earth climates in CCSM4, Climate of the Past, 8, 907–918, 2012a.

Yang, J., Peltier, W. R., and Hu, Y.: The initiation of modern "soft Snowball" and "hard Snowball" climates in CCSM3. Part II: Climate dynamic feedbacks, Journal of Climate, 25, 2737–2754, 2012b.

Zelinka, M. D., Myers, T. A., McCoy, D. T., Po-Chedley, S., Caldwell, P. M., Ceppi, P., Klein, S. A., and Taylor, K. E.: Causes of higher climate sensitivity in CMIP6 models, Geophysical Research Letters, 47, e2019GL085 782, https://doi.org/10.1029/2019GL085782, 2020.

Zhu, J. and Poulsen, C. J.: Last Glacial Maximum (LGM) climate forcing and ocean dynamical feedback and their implications for estimating climate sensitivity, Climate of the Past, 17, 253–267, https://doi.org/10.5194/cp-17-253-2021, 2021a.

Zhu, J. and Poulsen, C. J.: Last Glacial Maximum (LGM) climate forcing and ocean dynamical feedback and their implications for estimating climate sensitivity, Climate of the Past, 17, 253–267, 2021b.

Zhu, J., Otto-Bliesner, B. L., Brady, E. C., Poulsen, C. J., Tierney, J. E., Lofverstrom, M., and DiNezio, P.: Assessment of equilibrium climate sensitivity of the Community Earth System Model version 2 through simulation of the Last Glacial Maximum, Geophysical Research Letters, 48, e2020GL091 220, https://doi.org/10.1029/2020GL091220, 2021.

Zhu, J., Otto-Bliesner, B. L., Brady, E. C., Gettelman, A., Bacmeister, J. T., Neale, R. B., Poulsen, C. J., Shaw, J. K., McGraw, Z. S., and Kay, J. E.: LGM paleoclimate constraints inform cloud parameterizations and equilibrium climate sensitivity in CESM2, Journal of Advances in Modeling Earth Systems, 14, e2021MS002 776, 2022.

Appendix A: Snowball state under solar forcing and from LGM conditions

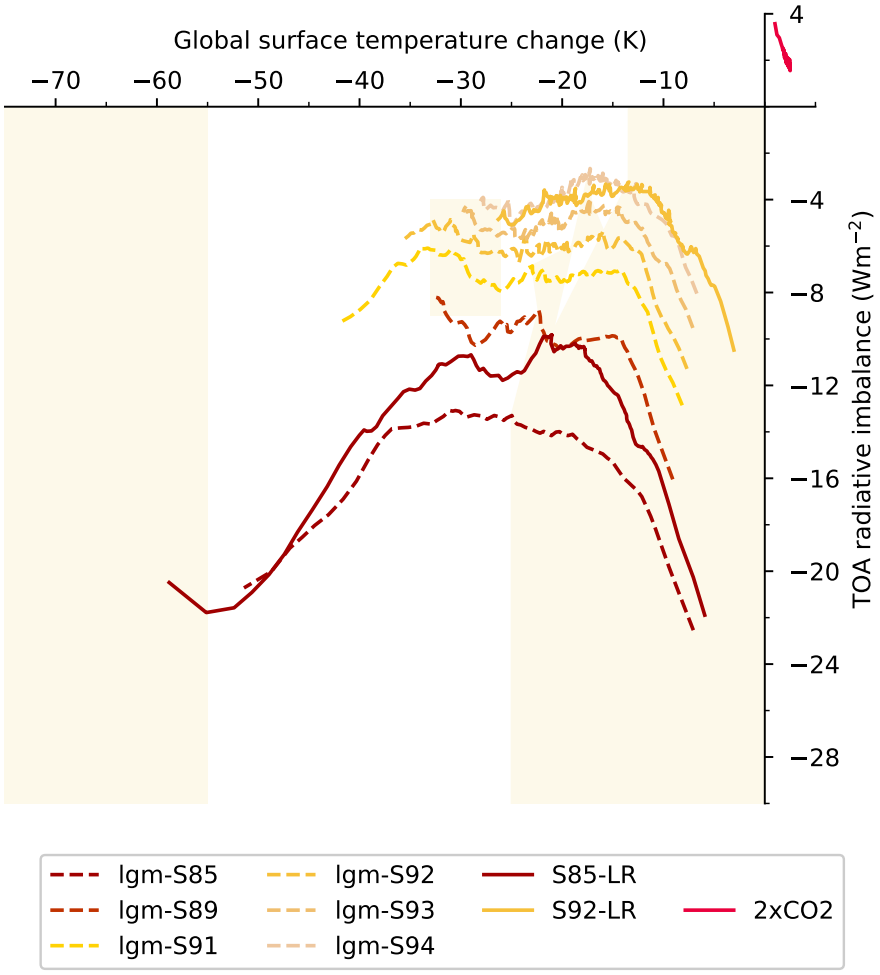

Figure A1. Top-of-atmosphere radiative imbalance (Wm^{-2}) versus global surface temperature anomaly with pre-industrial conditions (K) under solar forcing from LGM conditions. The similar phases of positive (white) and negative (colored) climate feedbacks as from PI conditions are shown.

We verify how snowball Earth transitions differ when starting from LGM or PI conditions. MPI-ESM1.2-LR is numerically unstable at low CO_2 concentrations, so we compare solar-forced snowball Earth transitions between LGM and PI instead.

The LGM is characterized by large ice sheets and lower sea-level which can affect cloud feedbacks as well as global circulations (Muglia and Schmittner, 2015; Sherriff-Tadano et al., 2018; Zhu and Poulsen, 2021a; Renoult et al., 2023), thus can influence the transition to a snowball Earth state. Changes in continental distribution and ocean areas are known to affect

inception temperatures. For instance, Voigt et al. (2011) indicates a snowball Earth transition at 96% of pre-industrial solar constant with Marinoan reconstructed paleogeography ($\sim$635 million years ago), which is characterized by agglomerated, bare-soil tropical continents, whereas it would require 94% or lower with PI continents. Tropical land masses reflect more radiations and therefore contribute substantially to snowball Earth transitions.

When initializing from LGM conditions (Fig. A1), the same main phases of negative and positive feedbacks are identified than from PI conditions. There are slight differences between both cases, for instance the LGM simulation show a single instability phase, whereas the runs starting from pre-industrial still display hints of multiple phases when the solar constant is set at 85% of PI value. However, the inception temperature connected to the main instability leading to the snowball Earth state happens at a broadly similar temperature than from PI conditions, between -15 K and -20 K relative to pre-industrial, which demonstrate the role of the feedback dependency on temperature, irrelevant of the differences in boundary conditions.

Memory effects are expected to differ from LGM and PI conditions and likely explain the slight differences in transition temperatures towards the snowball state. Indeed, the LGM ocean is colder than in PI, and the initial thermal state of the ocean is known to affect the speed at which the snowball state is reached (Bendtsen and Bjerrum, 2002). From the LGM, reaching snowball Earth is therefore easier, as tropical oceans are colder and the evacuation of heat via ocean mixing is enhanced. This should add further in rendering the LGM simulations difficult for modern climate models, as they usually initialise their experiments from LGM states of previous generations.

Appendix B: Additional figures

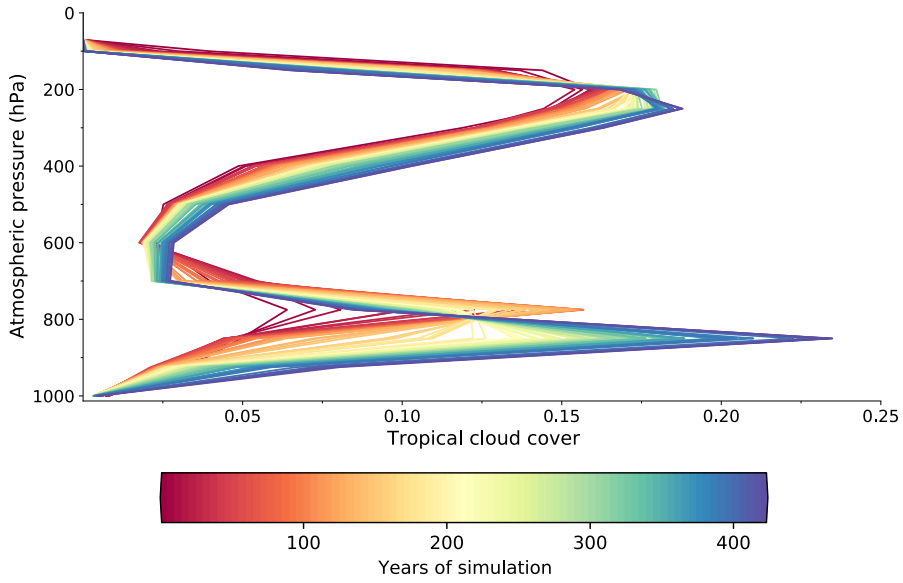

Figure B1. Evolution of tropical (30°s - 30°N) cloud cover within the first 15 K of cooling (425 years of simulation) in the 1/16xCO2 simulation.

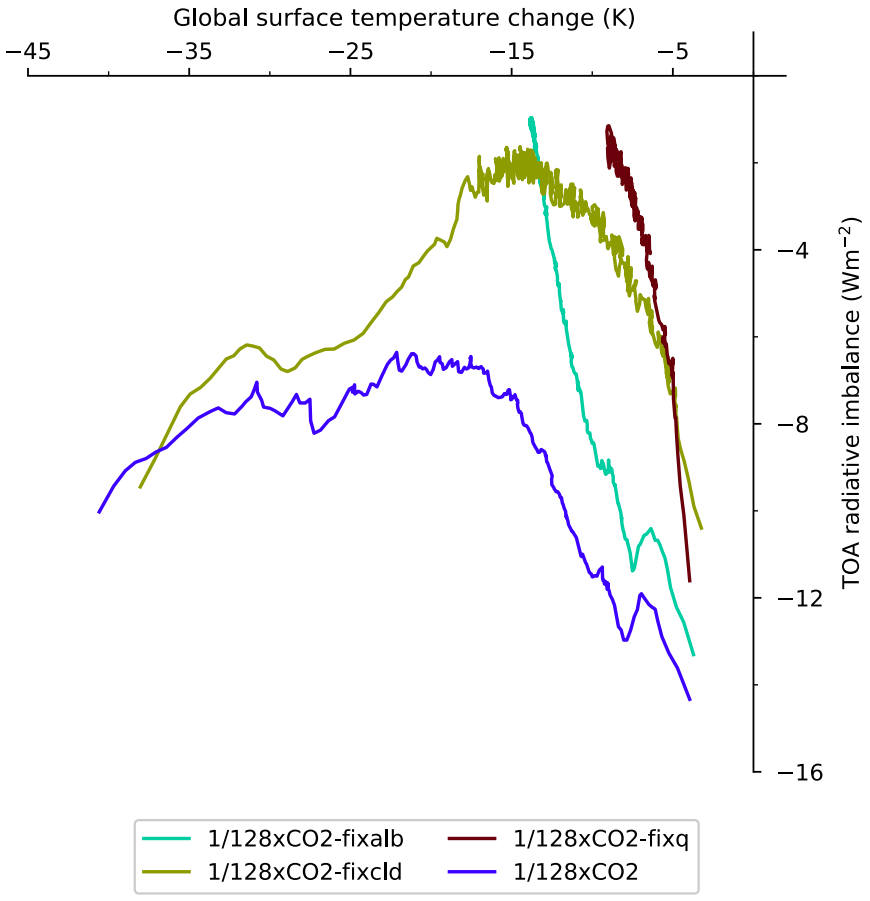

Figure B2. Top-of-atmosphere radiative imbalance (Wm^{-2}) versus global surface temperature anomaly with pre-industrial conditions (K) for the 1/128xCO2 simulation with either surface albedo (fixalb), water vapor (fixq) or cloud (fixcld) feedbacks locked to that of the control state.

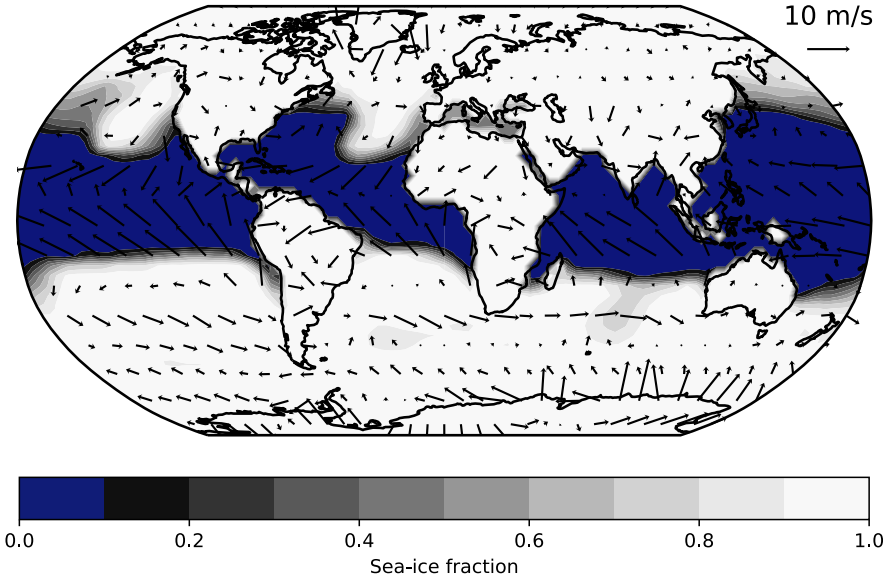

Figure B3. Surface wind field on sea-ice cover during the snowball Earth transition for the 1/16xCO2 simulation. Strong winds push sea ice equatorwards in the tropical regions.

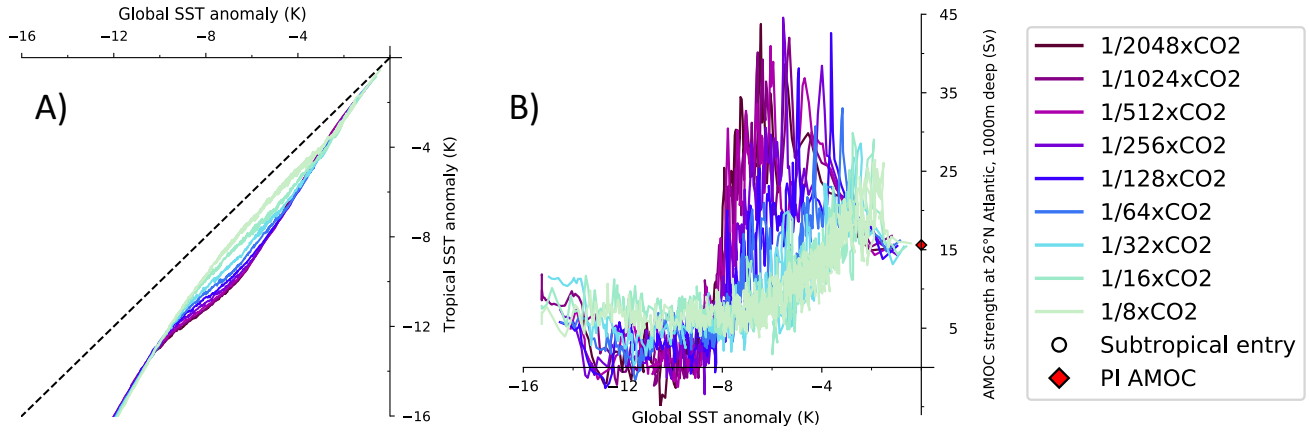

Figure B4. Analysis of tropical and global components affecting the rate of snowball Earth transitions. A) Differences in tropical and global SST cooling under all CO_2 forcing. B) Strength of the Atlantic meridional overturning circulation (AMOC) measured at 26°N, 1000 m deep (Sv) under all CO_2 forcing. The average pre-industrial AMOC strength, around 16 Sv, is highlighted.